Reprinted from THE PHYSICS OF FLUIDS VOLUME 6, NUMBER 6 JUNE 1963 *Printed in U.S.A.*

Predictions of the Structure of Radiation-Resisted Shock Waves

MAX. A. HEASLET AND BARRETT S. BALDWIN
National Aeronautics and Space Administration, Ames Research Center, Moffett Field, California

(Received 30 October 1962; revised manuscript received 25 January 1963)

The continuum, inviscid-flow equations of gas dynamics are used to predict the effect of thermal radiation on the internal structure of a shock wave. Numerical solutions of the governing equations show that considerable variation in the nature of the temperature and velocity profiles occurs, depending on the magnitude of the over-all velocity change and the relative strengths of the radiative and convective energy fluxes. A unique feature of the work is the demonstration that, for a range of parametric values, discontinuities necessarily arise in the temperature and velocity profiles. The results include: (a) numerical integration of the basic equations for a representative range of parameters; (b) an analytic study of the equations by means of expansion procedures; (c) a study of the uniqueness of the solutions; (d) proof that previously published investigations cannot be generally applicable since they are restricted to continuous solutions; (e) prediction within a strong shock of a temperature maximum considerably larger than that corresponding to the Rankine–Hugoniot conditions.

INTRODUCTION

THIS paper is concerned with the prediction of shock wave structure as influenced by one mode of energy dissipation. The continuum equations of one-dimensional gas dynamics, including energy transport by thermal radiation, are solved and the nature of the temperature and velocity profiles within shock waves is shown to have a strong dependence on two basic parameters. The work is a sequel to that of Clarke.[1] We are in disagreement with Clarke's results for a strong shock. All of his velocity and temperature profiles are continuous. In contrast we find that for sufficiently strong shocks an imbedded adiabatic shock always appears, and rather profound changes in the profiles arise. A similar discrepancy exists for weak shocks when the initial gas temperature is sufficiently low. In this case also a discontinuity corresponding to an imbedded adiabatic shock appears.

The effects of viscosity and heat conduction on shock thickness and structure have already been studied extensively. The early work of Taylor[2] and of Becker[3] establishes the analytic pattern of attack and the character of the profiles. The monographs by Hayes[4] and Lighthill[5] are each definitive treatments of the subject and provide a large number of references to allied work.

Aerodynamic studies of the effects of radiative energy flux are much more rare. Certainly, the gas temperatures encountered by practicing aerodynamicists have only recently become large enough to produce significant radiative interchange. Astrophysicists, on the other hand, have long been concerned with the contribution of radiation to the balance of momentum and energy in the interior of stars, but the temperatures encountered there are so great that the basic formulation of the problem is considerably different. The paper by Sen and Guess[6] treats the effect of radiation on shock structure, but is limited in application, since it treats only cases for which the absorption coefficient is large.

Attempts to analyze radiation-resisted shock waves in more general terms appear to have been initiated first by Prokof'ev[7] and by Clarke. Differences in the degree of complication of the gas model exist in the two papers but otherwise the analyses are similar in execution. In both cases, however, the discontinuous nature of the flow variable was not given adequate treatment. The present work was undertaken in an attempt to rectify the obvious mistakes in these papers. Two methods of attack were used: one based on a straightforward numerical study of the defining equations; one based on analytical expansion procedures. At the time our first calculations were being carried out on an IBM 7090, Professor R. Goulard called to our attention a paper by Zel'dovich[8] in which the work of Prokof'ev is

[1] J. F. Clarke, Phys. Fluids **5**, 1347 (1962).
[2] G. I. Taylor, Proc. Roy. Soc. (London) **A84**, 371 (1910).
[3] R. Becker, Z. Physik **8**, 321 (1922). Also NACA TM 505, 506 (1929).
[4] W. D. Hayes, *Gasdynamic Discontinuities*, Princeton Aeronautical Paperback No. 3 (Princeton University Press, Princeton, New Jersey, 1960).
[5] M. J. Lighthill, in *Surveys in Mechanics, G. I. Taylor, Anniversary Volume* (Cambridge University Press, London, 1956), p. 250.
[6] H. K. Sen and A. W. Guess, Phys. Rev. **108**, 560 (1957).
[7] V. A. Prokof'ev, Uch. Zap. Mosk. Gos. Univ. **172**, 79 (1952).
[8] Ia. B. Zel'dovich, Soviet Phys.—JETP **5**, 919 (1957).

discussed. The paper by Zel'dovich is primarily concerned with a proof of the existence of discontinuities for extreme cases but the methods used are adaptable to quantitative procedures. Parallelism also exists between our expansion procedures and approximate methods given in a paper by Raizer.[9] In retrospect, it thus appears that some duplication of effort occurred. In this presentation we have, however, empahsized the portions of our investigations that are new. The results include calculations for a complete range of parameters, analytical development of the expansion procedures, and a study of the uniqueness of the solutions and the monotonic character of the velocity profiles.

BASIC EQUATIONS

We consider the one-dimensional, steady flow of a gas with special regard for the effect of thermal radiation. In the absence of heat conductivity and viscosity, the conservation relations for mass, momentum, and energy become, respectively,

$$\frac{d}{dx}(\rho u) = 0, \tag{1a}$$

$$\rho u \frac{du}{dx} + \frac{dp}{dx} = 0, \tag{1b}$$

$$\rho u \frac{dh}{dx} - u \frac{dp}{dx} + \frac{d}{dx} q_r = 0, \tag{1c}$$

where p is pressure, ρ is density, u is gas velocity, h is specific enthalpy, and q_r is radiative heat flux. The contributions of radiative effects to pressure and enthalpy have been ignored.

Integration of Eqs. (1) yields

$$\rho u = \Gamma, \tag{2a}$$

$$\Gamma u + p = P = \Gamma c_1, \tag{2b}$$

$$\Gamma(h + \tfrac{1}{2}u^2) + q_r = E = \Gamma c_2, \tag{2c}$$

where Γ, P, E, c_1, and c_2 are constants of integration.

If subscripts 1 and 2 are used to denote, respectively, conditions at $x = -\infty$ and $x = +\infty$, we have

$$\Gamma = \rho_1 u_1 = \rho_2 u_2, \tag{3a}$$

$$P = \rho_1 u_1^2 + p_1 = \rho_2 u_2^2 + p_2, \tag{3b}$$

$$E = \rho_1 u_1 (h_1 + \tfrac{1}{2}u_1^2) = \rho_2 u_2 (h_2 + \tfrac{1}{2}u_2^2). \tag{3c}$$

These latter relations are, in fact, the Rankine–Hugoniot conditions that are satisfied in passage through a shock wave.

The simplifying assumption that the gas is a perfect one does not modify essentially the topology of the shock structure. We therefore introduce the relations

$$p = R\rho T, \qquad h = c_p T, \qquad R = c_p - c_v, \qquad \gamma = c_p/c_v, \tag{4}$$

where R is the gas constant and γ the ratio of specific heats at constant pressure and volume, is also a constant. Equations (2b) and (2c) then reduce to

$$RT = (c_1 - u)u, \tag{5a}$$

$$u^2 - \frac{2\gamma}{\gamma + 1} c_1 u + \frac{2(\gamma - 1)}{(\gamma + 1)} c_2 = \frac{2(\gamma - 1)}{\Gamma(\gamma + 1)} q_r. \tag{5b}$$

The appropriate expression for radiative flux in an absorbing and emitting gray gas is best expressed as a function of the dimensionless distance η defined by

$$\eta = \int_0^x \alpha(x_1)\, dx_1, \tag{6}$$

where $\alpha(x)$ is the local absorption coefficient; see e.g., Kourganoff.[10] One has

$$q_r(\eta) = 2 \int_{-\infty}^{\infty} \sigma T^4(\eta_1) \operatorname{sgn}(\eta - \eta_1) E_2(|\eta - \eta_1|)\, d\eta_1, \tag{7}$$

where σ is the Stefan–Boltzmann constant and the function $E_2(\eta)$ is the integro-exponential function of order 2. It may also be noted, parenthetically, that q_r is defined so that flux is positive when the flow of energy is in the positive x or η direction; the sign terminology is thus opposite to the convention employed by astrophysicists.

A final approximation is now made by writing

$$E_2(\eta) \approx m e^{-n\eta}, \tag{8}$$

where m and n are chosen by somewhat arbitrarily imposed fitting techniques. Vincenti and Baldwin[11] have proposed the values

$$m = \tfrac{1}{3}n^2, \qquad n = 1.562, \tag{9}$$

which follow from imposing the requirements that the solution be exact in the Rosseland limit of strong absorption and that the approximate expression in Eq. (8) be a least square fit to $E_2(\eta)$. Here, we shall introduce the new variable ξ, where

$$\xi = n\eta \tag{10}$$

[9] Iu. P. Raizer, Soviet Phys.—JETP 5, 1242 (1957).

[10] V. Kourganoff, *Basic Methods in Transfer Problems* (Clarendon Press, Oxford, England, 1952).

[11] W. G. Vincenti and B. S. Baldwin, Jr., J. Fluid Mech. 12, 449 (1962).

so that no explicit dependence on n will appear in the kernel function of the governing integral equation; see Eq. (13) below. Then the results in terms of ξ will apply for any choice of the constants m and n in Eq. (8).

Equations (5a) and (5b) are now to be recast with ξ as independent variable. Setting, first,

$$v(\xi) = u(x)/c_1, \tag{11}$$

we have

$$T = (c_1^2/R)(v - v^2), \tag{12a}$$

$$v^2 - \frac{2\gamma}{(\gamma+1)}v + \frac{2(\gamma-1)}{(\gamma+1)}\frac{c_2}{c_1^2} = \frac{4m(\gamma-1)\sigma c_1^6}{\Gamma(\gamma+1)nR^4} \cdot \int_{-\infty}^{\infty} [v(\xi_1) - v^2(\xi_1)]^4 \operatorname{sgn}(\xi - \xi_1) e^{-|\xi-\xi_1|}\, d\xi_1. \tag{12b}$$

Equations (12a) and (12b) correspond precisely to Clarke's idealization of the shock structure problem and are cast in a terminology easily related to his. Clarke furthermore sets $[32m(\gamma - 1)\sigma c_1^6]/[\Gamma(\gamma + 1)R^4] = C$ but for convenience we introduce $K(=C/n)$. Formal simplification of Eq. (12b) is also achieved through introduction of the following:

$$v_1 = u_1/c_1, \qquad v_2 = u_2/c_1.$$

The Rankine–Hugoniot relations then permit us to write (12b) as

$$-(v_1 - v)(v - v_2) = \frac{K}{8}\int_{-\infty}^{\infty} (v - v^2)^4 \operatorname{sgn}(\xi - \xi_1) e^{-|\xi-\xi_1|}\, d\xi_1. \tag{13}$$

Equation (13) is the governing integral equation that must be solved.

Two speeds of sound play important roles in the analysis of wave structure, namely, the isothermal and isentropic speeds a_t and a_s. We have the defining relations

$$a_t^2 = RT = p/\rho, \qquad a_s^2 = \gamma a_t^2, \tag{14}$$

when

$$u = a_t, \qquad v = \tfrac{1}{2}, \tag{15a}$$

$$u = a_s = \tfrac{1}{2}(u_1 + u_2) = \frac{\gamma}{(\gamma+1)}c_1, \qquad v = \frac{\gamma}{\gamma+1} = \frac{v_1 + v_2}{2}. \tag{15b}$$

From Eq. (15b) it follows that $u_1 \geq a_s \geq u_2$ so that at some value of ξ the shock velocity takes on the value a_s. We arbitrarily fix this position at $\xi = 0$.

Reduction to Differential Equation

Mathematical analysis of Eq. (13) must cope with at least three major difficulties. First, the nonlinearity prevents straightforward use of many standard techniques of solution; second, the length of the region of integration being of infinite extent the equation must be classified as a singular one which again precludes access to some methods involving mean value relations; finally, the smoothing effect of the integration in the right member transforms discontinuous functions into continuous functions. We know, for example, that $(v_1 - v)(v - v_2)$ must be continuous since it is proportional to radiative flux, but we have no *a priori* knowledge that $(v - v^2)^4$, or v, undergoes no discontinuity. We must, in fact, leave the continuity of these latter functions open to question since the gas is assumed inviscid and the absence of heat conductivity leaves the continuity of $(v - v^2)^4$ αT^4 in doubt.

Subsequent results will show that discontinuities do occur corresponding to imbedded inviscid shocks. For that reason it is expedient to introduce a continuous dependent variable in place of v. At the same time a proper choice of the variable to be used leads to a simple parametric representation for all possible imbedded shocks. The variable $\theta(\xi)$ is therefore introduced where

$$\theta(\xi) = [\gamma/(\gamma + 1) - v]^2. \tag{16}$$

Since $\theta(\xi) = \frac{1}{4}(v_1 - v_2)^2 - (v_1 - v)(v - v_2)$, the continuity of $\theta(\xi)$ is established. The zero value of ξ has been set so that

$$v > \gamma/(\gamma+1), \quad \xi < 0; \qquad v < \gamma/(\gamma+1), \quad \xi > 0;$$

assuming that $v(\xi)$ is monotonic. Hence Eq. (16) gives

$$v(\xi) = \gamma/(\gamma+1) - (\operatorname{sgn}\xi)[\theta(\xi)]^{\frac{1}{2}}. \tag{17}$$

Equation (13) then becomes

$$\theta(\xi) = \theta_\infty + \tfrac{1}{2} \cdot \int_{-\infty}^{\infty} F[\theta(\xi_1)] \operatorname{sgn}(\xi - \xi_1) e^{-|\xi-\xi_1|}\, d\xi_1, \tag{18a}$$

where

$$F(\theta) = \frac{K}{4}\left[\frac{\gamma}{(\gamma+1)^2} + \left(\frac{\gamma-1}{\gamma+1}\right)(\operatorname{sgn}\xi)\theta^{\frac{1}{2}} - \theta\right]^4, \tag{18b}$$

$$\theta_\infty = \tfrac{1}{4}(v_1 - v_2)^2. \tag{18c}$$

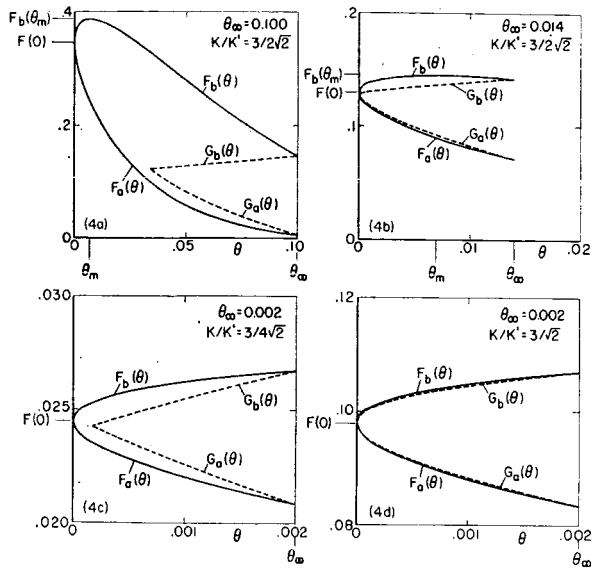

FIG. 1. The functions $F(\theta)$ and $G(\theta)$.

Equation (18) can be replaced by a differential form. Taking derivatives with respect to ξ, we get the following relations:

$$\frac{d\theta}{d\xi} = F - \frac{1}{2}\int_{-\infty}^{\infty} F[\theta(\xi_1)]e^{-|\xi-\xi_1|}\,d\xi_1, \tag{19a}$$

$$\frac{d^2\theta}{d\xi^2} = \frac{dF}{d\theta}\frac{d\theta}{d\xi} + \frac{1}{2} \cdot \int_{-\infty}^{\infty} F[\theta(\xi_1)]\,\mathrm{sgn}\,(\xi - \xi_1)e^{-|\xi-\xi_1|}\,d\xi_1, \tag{19b}$$

$$\frac{d^2\theta}{d\xi^2} - (\theta - \theta_\infty) = \frac{dF}{d\theta}\frac{d\theta}{\theta\xi}, \tag{19c}$$

where $F(\theta)$ is defined as in Eq. (18b). Equation (19c) is the desired differential equation. An alternative form with which we shall be directly concerned is

$$\frac{dG(\theta)}{d\theta} = (\theta_\infty - \theta)\frac{1}{d\theta/d\xi}, \tag{20a}$$

where

$$G(\theta) = F(\theta) - d\theta/d\xi. \tag{20b}$$

It is important to remark that $G(\theta)$, defined in Eq. (20b), is also a continuous function of θ and ξ. That this is so, follows directly from Eq. (19a) since G is given by the integral term in the right member which is everywhere continuous. $G(\theta)$ has two branches, $G_a(\theta)$ and $G_b(\theta)$, corresponding to the two branches of $F(\theta)$. The subscripts a and b are used to denote conditions ahead of and behind the shock midpoint at $\xi = 0$.

The boundary conditions associated with $G(\theta)$ can be deduced from Eqs. (19c) and (20b) using the fact that derivatives with respect to ξ are zero at the end points ($\xi = \pm\infty$). The boundary conditions are at $\xi = -\infty$:

$$\theta = \theta_\infty, \qquad G = F_a(\theta_\infty), \tag{20c}$$

at $\xi = +\infty$:

$$\theta = \theta_\infty, \qquad G = F_b(\theta_\infty). \tag{20d}$$

Since $G(\theta)$ starts out in the a branch at $\xi = -\infty$, and ends up in the b branch at $\xi = +\infty$, a transition from one branch to the other must occur at some intermediate point. Since G and θ are each continuous functions of ξ, and hence $G(\theta)$ continuous, the transition from the a to the b branch must occur at a point where $G_a(\theta)$ equals $G_b(\theta)$. It can be shown that the previous choice of the zero point on the ξ scale corresponds to the point where $G_a(\theta)$ equals $G_b(\theta)$.

The integrations to get the two branches of $G(\theta)$ are conveniently started from the extreme points corresponding to $\xi = \pm\infty$. Once the values of $G_a(\theta)$ and $G_b(\theta)$ are known, the quantity $d\theta/d\xi$ can be evaluated from Eq. (20b) and the result integrated to obtain θ as a function of ξ. The velocity profile can then be found by substitution in Eq. (17). The results from the numerical integration for $G(\theta)$ in several representative cases are shown in Fig. 1. The value K' appearing in the labels is defined as $K' = 2\sqrt{2}(\gamma + 1)^7\theta_\infty^{\frac{1}{2}}/\gamma^3(\gamma - 1)$. Its significance will be developed in more detail in a later section.

Clarke's solution can be paraphrased by discussing it in terms of the present variables instead of the ones he actually used. Since his velocity profiles are continuous, the transition from the a to the b branch is made at $\theta = 0$ [see Eq. (17)]. For the case shown in the upper left plot of Fig. 1, Clarke's solution would correspond to continuing the G_a and G_b curves beyond the point of intersection, all the way to $\theta = 0$. Since G_a is not equal to G_b at $\theta = 0$ for this case, the condition that $G(\theta)$ must be continuous is violated by his solution. In the special cases where $G_a(\theta)$ is equal to $G_b(\theta)$ at $\theta = 0$ (the right-hand plots in Fig. 1) Clarke's solution is correct.

Results from numerical integration. The curves in Fig. 1 were drawn from calculations and integrations carried out on an electronic computer. In all cases the value $\gamma = \frac{7}{5}$ was used, rather than a smaller

number, in order to illustrate the variations better. Other constant values of γ would lead to qualitatively similar results. The parameter θ_m appearing in the upper two plots of Fig. 1 is the value of θ where $F_b(\theta)$ has a maximum and can be expressed in terms of γ by the relation $\theta_m = (\gamma - 1)^2/4(\gamma + 1)^2$.

Figure 2 shows the details of the profiles as functions of ξ. Each of the nine subplots contains three profiles: The dimensionless velocity $v(=u/c_1)$, along with the dimensionless temperature function $\tilde{T}$ and the flux function $\tilde{q}$ where

$$\tilde{T} = RT/c_1^2 = v - v^2, \tag{21a}$$

$$\tilde{q} = \frac{\theta_\infty - \theta}{\theta_\infty} = 4\frac{(v_1 - v)(v - v_2)}{(v_1 - v_2)^2}. \tag{21b}$$

Nine combinations of parameters were chosen in order to give representative variations of predicted shapes. The values $\theta_\infty = 0.002$, 0.025, and 0.100 correspond, respectively, to a weak shock, a wave of intermediate strength, and a strong shock. As will be explained shortly, the value $K = (\frac{3}{2}\sqrt{2})K'$ determines roughly the dividing line between discontinuous and continuous profiles, when continuity is not precluded by a large value of θ_∞. Accordingly, K is expressed in units of this particular value and K/K' is given small, intermediate, and large values. Radiative effects are necessarily small when $K/K' \ll 1$.

It follows from the definition of ξ, Eqs. (10) and (6), that $\xi = 1.0$ corresponds roughly to a distance of one local radiation mean free path length. If the temperature varies appreciably through the wave, the radiation mean free path varies, and the profiles in terms of actual physical distances are distorted from the shapes given in Fig. 2. We shall limit our considerations here to the reduced variable ξ and thus are able to avoid specifying the dependence of the absorption coefficient on temperature.

In the top row, the strong shock differs only slightly from a classical inviscid shock when radiation is weak. The small variations in v and $\tilde{T}$ that do occur die out in essentially one radiation mean free path length ahead of and behind the imbedded inviscid shock. The radiative flux $\tilde{q}$ is symmetric about $\xi = 0$ and goes to zero in the regions where v and $\tilde{T}$ become constant. As the radiation parameter K is increased, the variations in v and $\tilde{T}$ ahead

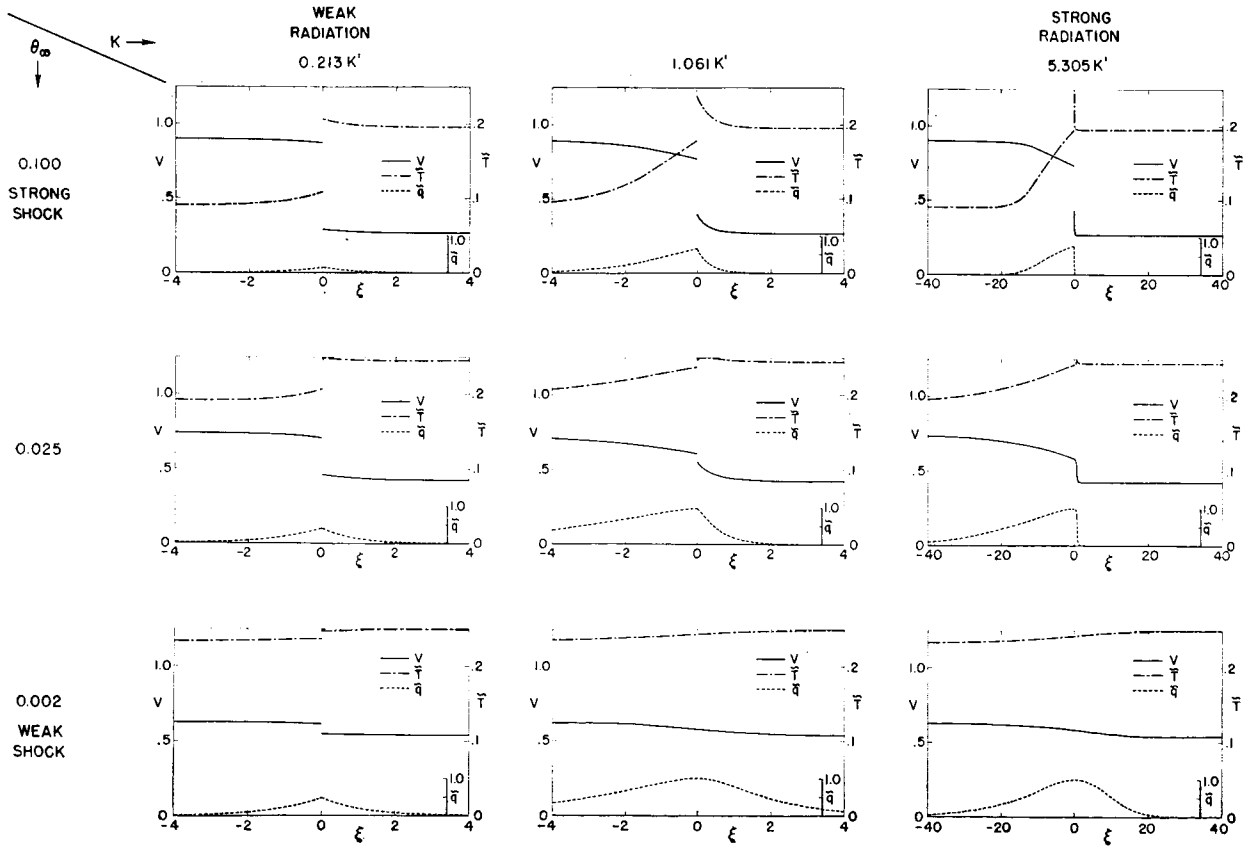

FIG. 2. Profiles of dimensionless velocity V, temperature $\tilde{T}$, and heat flux $\tilde{q}$.

of and behind the imbedded shock increase in magnitude. The values of $\tilde{q}$ also increase and an asymmetry develops. For large K the variations ahead extend over many radiation mean free path lengths, and the variations behind become compressed into a small fraction of a radiation path length. In all three subplots of the top row, there is a nonzero radiative flux q through the imbedded shock. Nevertheless, the discontinuities correspond to *adiabatic* inviscid shocks because there can be no radiation from nor absorption in a gas layer of vanishing thickness.

The results for an intermediate shock strength in the middle row of Fig. 2 reveal trends similar to those for a strong shock. In this case the temperature profile develops a small peak behind the imbedded shock. At large K, the profiles become continuous and are in agreement with the results of Clarke.

The bottom row gives results for a weak wave. The trends with increasing K for the forward part of the profiles are similar to those for the previous cases. However, the rear part behaves differently in that it also becomes greatly dispersed for large K rather than being compressed as is the case for the stronger waves. An explanation of this difference is arrived at by means of an expansion of the solution for large K, derived in the next section. In a weak wave, the transition from discontinuous to continuous profiles occurs at a smaller value of K/K' than for stronger waves. The temperature maximum within the wave, which appears for stronger shocks, is absent in the weak waves.

It should be noted that $\tilde{q} = (\theta_\infty - \theta)/\theta_\infty$ is normalized through division by the strength of the wave, $\theta_\infty = \frac{1}{4}(v_1 - v_2)^2$. As a result, the relative magnitudes of q in different subplots have significance only when θ_∞ is held fixed. We see that for a wave of fixed strength, the radiative flux $\tilde{q}$ does not increase indefinitely with increasing K. Instead, the peak value levels off and is nearly constant when K exceeds K'.

FURTHER ANALYTICAL CONSIDERATIONS

Since the conclusions in the previous section are to some extent dependent on the accuracy of numerical procedures, it is of interest to determine whether any general information can be inferred analytically. It is possible to show that discontinuities must occur in the profiles when the shock is sufficiently strong and also when the radiation is sufficiently weak. By means of expansion procedures a closed-form solution can be found for the case of weak radiation, and an interesting singular perturbation effect is found in the Rosseland limit of strong absorption.

Values of the Parameters at which Discontinuities Must Occur

Assuming that $v(\xi)$ decreases monotonically (see Appendix), we infer from Eq. (17)

$$d\theta/d\xi \leq 0, \qquad \xi < 0, \tag{22a}$$

$$d\theta/d\xi \geq 0, \qquad \xi > 0. \tag{22b}$$

It then follows from Eq. (20b) that

$$G_a(\theta) \geq F_a(\theta), \qquad G_b(\theta) \leq F_b(\theta). \tag{23a}$$

Also, since $\theta_\infty > \theta$ if v is monotonic, Eq. (20a) indicates

$$dG_a(\theta)/d\theta < 0, \qquad dG_b(\theta)/d\theta > 0. \tag{23b}$$

Thus both branches of $G(\theta)$ lie within the branches of $F(\theta)$ and are monotonic oppositely. It follows that G_a and G_b cannot intersect at more than one point. Since the transition from G_a to G_b must occur at G_a equal to G_b, the solution is unique, if it exists.

It is not necessary to carry out the integration in order to prove that the velocity profile is discontinuous in many cases. Consider, first, the case typified by the upper left plot in Fig. 1. Here $\theta_\infty > 4\theta_m = [(\gamma - 1)/(\gamma + 1)]^2$ and $F_b(\theta_\infty) \leq F(0)$ [see Eq. (18b)]. Since $G_b(\theta)$ lies always below $F(0)$, the branch $G_a(\theta)$ must intersect $G_b(\theta)$ before θ reaches zero.

It is also possible to prove that the velocity profile cannot be continuous if K is sufficiently small. To show this assume continuity and expand Eqs. (20a, b) about $\theta = 0$ as follows:

$$F_a(\theta) = F(0) - C\theta^{\frac{1}{2}} + \cdots, \tag{24a}$$

$$F_b(\theta) = F(0) + C\theta^{\frac{1}{2}} + \cdots, \tag{24b}$$

where

$$C = [\gamma^3(\gamma - 1)K]/(\gamma + 1)^7. \tag{25}$$

Since the two branches of $G(\theta)$ lie between the two branches of $F(\theta)$, it follows that

$$G_a(\theta) = F(0) - A\theta^s + \cdots, \tag{26a}$$

$$G_b(\theta) = F(0) + B\theta^t + \cdots, \tag{26b}$$

where

$$0 < s, t \leq \tfrac{1}{2}, \qquad A, B > 0.$$

Elimination of $d\theta/d\xi$ from Eqs. (20a, b) and substitution of Eqs. (24) and (25) leads to the results

$$s = t = \tfrac{1}{2}, \qquad B = A,$$

and A must satisfy the equation

$$A^2 - CA + 2\theta_\infty = 0,$$

or

$$A = \tfrac{1}{2}C \pm [(\tfrac{1}{2}C)^2 - 2\theta_\infty]^{\frac{1}{2}}.$$

A real value of A will be obtained only if

$$\tfrac{1}{2}C > 2^{\frac{1}{2}}\theta_\infty$$

or

$$K > [2^{\frac{3}{2}}(\gamma + 1)^7\theta_\infty^{\frac{1}{2}}]/[\gamma^3(\gamma - 1)] \equiv K'. \qquad (27)$$

We conclude that for $K < K'$, a continuous solution does not exist.

The preceding discussion enables us to limit drastically the range of parameters for which continuous velocity profiles may possibly occur. The shaded regions in Fig. 3 correspond to cases for which a discontinuous profile *must* occur; that is, when $K < K'$ or

$$\left(\frac{v_1 - v_2}{2}\right)^2 = \theta_\infty > 4\theta_m = \left(\frac{\gamma - 1}{\gamma + 1}\right)^2.$$

By a more detailed investigation of the solution near $\theta = 0$, it can be shown that discontinuous profiles must occur for $K < (\frac{3}{2}\sqrt{2})K'$ when θ_∞ is sufficiently small. Also, by establishing a closed-form lower bound on G_a and an upper bound on G_b, discontinuous behavior is seen to persist for values of θ_∞ somewhat less than $4\theta_m$. Thus the shaded areas in Fig. 3 could be extended further into the unshaded area than is indicated in the figure. The exact positions of the dividing lines for values of the parameters leading to discontinuous or continuous profiles have not been determined.

Closed-Form Solutions for Limiting Cases

The method of solution indicated in the previous sections can be further illustrated by closed-form analysis of the limiting cases corresponding to $K \ll K'$ and $K \gg K'$. For this purpose, it is convenient to introduce the following functions to replace $F(\theta)$ and $G(\theta)$:

$$f(\theta) = F(\theta)/K = \tfrac{1}{4}\{\tfrac{1}{4} - [\theta_m^{\frac{1}{2}} - (\operatorname{sgn}\xi)\theta^{\frac{1}{2}}]^2\}^4, \qquad (28)$$

$$g(\theta) = G(\theta)/K. \qquad (29)$$

In contrast to the behavior of $F(\theta)$, the function $f(\theta)$ remains finite and nonzero for limiting values of K. The function $g(\theta)$ also has these properties since, as previously noted, the two branches of $G(\theta)$ lie between the two branches of $F(\theta)$ in the region of interest, see Eq. (23). Since f and g differ from F and G only by the multiplicative constant K, all of the foregoing equations and properties of the latter functions can be easily applied in terms of f and g. The governing Eqs. (20a, b) can be written as

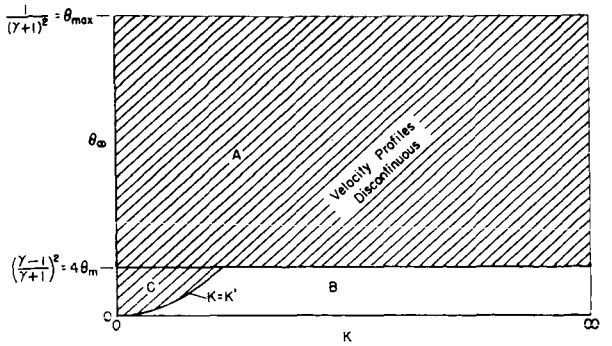

FIG. 3. Values of the parameters at which discontinuous profiles must occur.

$$K\frac{d\theta}{d\xi}\frac{dg}{d\theta} = \theta_\infty - \theta, \qquad (30a)$$

$$g(\theta) = f(\theta) - (d\theta/d\xi)/K. \qquad (30b)$$

Combination of these yields the single equation

$$K^2(f - g)\, dg/d\theta = \theta_\infty - \theta \qquad (31)$$

for the unknown function $g(\theta)$. The boundary conditions are, from Eqs. (20c, d)

$$g_a(\theta_\infty) = f_a(\theta_\infty), \qquad g_b(\theta_\infty) = f_b(\theta_\infty). \qquad (32)$$

It may be recalled that the subscript a refers to the branch of sgn $(\xi)\theta^{\frac{1}{2}}$ corresponding to $\xi < 0$ and the subscript b refers to $\xi > 0$.

Expansion for small K. Specializing to the case of small K, one concludes from Eq. (31) that the magnitude of $dg/d\theta$ is very large, because the magnitudes of the other quantities appearing in that equation do not go to infinity or zero as K goes to zero. Since the slopes of $g_a(\theta)$ and $g_b(\theta)$ are very steep, they must intersect at a value of θ near the starting value θ_∞ (see Fig. 1, lower left). Then to lowest order in K, $f(\theta) \approx f(\theta_\infty)$ and Eq. (31) can be written as

$$[f(\theta_\infty) - g(\theta)]\frac{d}{d\theta}[f(\theta_\infty) - g(\theta)] = \frac{\theta - \theta_\infty}{K^2} + [f(\theta_\infty) - f(\theta)]\frac{d}{d\theta}[f(\theta_\infty) - g(\theta)]. \qquad (33)$$

To the lowest order in K, the last term on the right can be neglected. A systematic expansion to any order in K follows from substitution of the previous approximation in the right side of Eq. (33) and

integration of the resulting equation. We find

$$g_a(\theta) = f_a(\theta_\infty) + (\theta_\infty - \theta)/K + O(K), \quad (34a)$$

$$g_b(\theta) = f_b(\theta_\infty) - (\theta_\infty - \theta)/K + O(K). \quad (34b)$$

Once $g_a(\theta)$ and $g_b(\theta)$ are known, θ as a function of ξ follows from Eq. (30a). Neglecting terms of order K in Eqs. (34a, b), we obtain

$$(d\theta/d\xi)_a = -(\theta_\infty - \theta) + O(K^2), \quad (35a)$$

$$(d\theta/d\xi)_b = (\theta_\infty - \theta) + O(K^2). \quad (35b)$$

It has previously been shown that $\xi = 0$ at $\theta = \theta_0$, the point of intersection of g_a and g_b. From Eqs. (34a, b), θ_0 is given by

$$\theta_0 = \theta_\infty - \tfrac{1}{2}K[f_b(\theta_\infty) - f_a(\theta_\infty)] + O(K^2).$$

Integration of Eqs. (35a, b) leads to

$$\xi_a = -\int_{\theta_0}^{\theta} \frac{d\theta_1}{\theta_\infty - \theta_1} = \ln\left(\frac{\theta_\infty - \theta}{\theta_\infty - \theta_0}\right) + O(K^2),$$

$$\xi_b = \int_{\theta_0}^{\theta} \frac{d\theta_1}{\theta_\infty - \theta_1} = \ln\left(\frac{\theta_\infty - \theta_0}{\theta_\infty - \theta}\right) + O(K^2),$$

and the solution for $\theta(\xi)$ is

$$\theta = \theta_\infty - \tfrac{1}{2}K[f_b(\theta_\infty) - f_a(\theta_\infty)]e^{-|\xi|} + O(K^2). \quad (36)$$

The dimensionless velocity, temperature, and flux profiles are now found by substitution from Eq. (36) into Eqs. (17) and (21a, b). The results are

$$v = \frac{\gamma}{\gamma+1} - \theta_\infty^{\frac{1}{2}}(\operatorname{sgn}\xi) + \frac{K}{4}\left[\frac{f_b(\theta_\infty) - f_a(\theta_\infty)}{\theta_\infty^{\frac{1}{2}}}\right] \cdot(\operatorname{sgn}\xi)e^{-|\xi|} + O(K^2), \quad (37a)$$

$$\tilde{T} = \tfrac{1}{4} - [\theta_m^{\frac{1}{2}} - (\operatorname{sgn}\xi)\theta_\infty^{\frac{1}{2}}]^2 + \frac{K}{2}\left[\frac{f_b(\theta_\infty) - f_a(\theta_\infty)}{\theta_\infty^{\frac{1}{2}}}\right] \cdot[\theta_\infty^{\frac{1}{2}} - (\operatorname{sgn}\xi)\theta_m^{\frac{1}{2}}]e^{-|\xi|} + O(K^2), \quad (37b)$$

$$\tilde{q} = \frac{K}{2}\left[\frac{f_b(\theta_\infty) - f_a(\theta_\infty)}{\theta_\infty}\right]e^{-|\xi|} + O(K^2). \quad (37c)$$

In terms of the initial and final values of velocity and temperature, these become

$$v = \left(\frac{v_1 + v_2}{2}\right) - \left(\frac{v_1 - v_2}{2}\right)(\operatorname{sgn}\xi) + \frac{K}{8}\left(\frac{\tilde{T}_2^4 - \tilde{T}_1^4}{v_1 - v_2}\right)(\operatorname{sgn}\xi)e^{-|\xi|} + O(K^2), \quad (38a)$$

$$\tilde{T} = \left(\frac{\tilde{T}_2 + \tilde{T}_1}{2}\right) + \left(\frac{\tilde{T}_2 - \tilde{T}_1}{2}\right)(\operatorname{sgn}\xi) + \frac{K}{8}\left(\frac{\tilde{T}_2^4 - \tilde{T}_1^4}{v_1 - v_2}\right)\left[v_1 - v_2 - \left(\frac{\gamma-1}{\gamma+1}\right)(\operatorname{sgn}\xi)\right] \cdot e^{-|\xi|} + O(K^2), \quad (38b)$$

$$\tilde{q} = \frac{K}{2}\left[\frac{\tilde{T}_2^4 - \tilde{T}_1^4}{(v_1 - v_2)^2}\right]e^{-|\xi|} + O(K^2). \quad (38c)$$

Equations (37) and (38) apply for waves of any strength when K is sufficiently small. For $K = 0$, we have an adiabatic inviscid shock. As K increases, for a fixed strength of the over-all wave, the imbedded adiabatic inviscid shock strength is reduced and the transitions to the initial and final conditions follow exponential variations. The results for $K = 0.213\,K'$ plotted in Fig. 2 are given quite accurately by Eqs. (37). These equations indicate that for small K, the over-all shock thickness is of the order of the sum of the radiation mean free paths in the regions ahead of and behind the inner shock.

In the expansion for $K \gg K'$, three distinct cases arise, depending on the value of θ_∞ relative to the parameter $\theta_m = (\gamma - 1)^2/4(\gamma + 1)^2$.

Case I, large K, weak shock ($\theta_\infty < \theta_m$). Equation (31) shows that in the limit as K goes to infinity, either $g = f(\theta)$ or $dg/d\theta = 0$. The choice between these possibilities is made by imposing the requirements that g_a and g_b be monotonic oppositely and lie between the two branches of $f(\theta)$. For the present case it can be established that $g \to f(\theta)$ as $K \to \infty$, and Eq. (31) is rewritten as

$$[f(\theta) - g]\frac{df}{d\theta} = \frac{\theta_\infty - \theta}{K^2} + \frac{1}{2}\frac{d}{d\theta}[f(\theta) - g]^2. \quad (39)$$

To lowest order in K^{-1}, the last term on the right can be neglected. Higher approximations can be found by substituting the previous approximation in the right side and integrating the result. By this process, we obtain

$$g(\theta) = f(\theta) - \frac{\theta_\infty - \theta}{K^2(df/d\theta)} + O(K^{-4}). \quad (40)$$

As in the case of small K, the solution in terms of θ can be converted to a solution in terms of ξ by the use of Eq. (30a). The results are

$$\xi_a(\theta) = K\int_0^{\theta} \frac{df_a(\theta_1)/d\theta_1}{\theta_\infty - \theta_1}\,d\theta_1 + O(K^{-1}), \quad (41a)$$

$$\xi_b(\theta) = K\int_0^{\theta} \frac{df_b(\theta_1)/d\theta_1}{\theta_\infty - \theta_1}\,d\theta_1 + O(K^{-1}), \quad (41b)$$

These integrals start at $\theta = 0$, for sufficiently large K, because the two branches of $g(\theta)$ intersect at $\theta = 0$. The appearance of the factor K in Eqs. (41a, b) indicates that, for large K, the radiation resisted shock thickness is proportional to K and hence is large compared to the radiation mean free path. The results from these equations were compared with the numerical results of Fig. 2 for

$\theta_\infty = 0.002\ K = 5.305\ K'$ and were found to provide a very good approximation at that value of K.

Case II, large K, intermediate shock strength ($\theta_m < \theta_\infty < 4\theta_m$). The solution for $f_a(\theta)$ in this case is the same as for the previous one. The solution for $f_b(\theta)$ involves three separate expansions for small, intermediate, and large θ. The results are rather complicated and will not be given here. However, it is of interest to note that calculations based on the expansion agree quite closely with those from the machine computations at a value of $K = 5.305\ K'$ corresponding to the middle right plot in Fig. 2.

Case III, large K, strong shock ($4\theta_m < \theta_\infty$). Figure 4 is a plot of f and g obtained numerically for $\gamma = \frac{7}{5}$, $\theta_\infty = 0.1$, $K = 5.305\ K'$, corresponding to the upper right plot in Fig. 2. It is apparent that the first term on the right in Eq. (40) provides a good approximation for $g_a(\theta)$. Equation (41a) is also accurate at these values of the parameters. However the choice $g_b(\theta) \to f_b(\theta_\infty)$ must be made here rather than $g_b(\theta) \to f_b(\theta)$. The appropriate rearrangement of Eq. (31) for expansion to higher order is

$$[f_b(\theta) - f_b(\theta_\infty)]\frac{dg_b}{d\theta} = \frac{\theta_\infty - \theta}{K^2} + [g_b(\theta) - f_b(\theta_\infty)]\frac{dg_b}{d\theta}. \tag{42}$$

To lowest order in K^{-1}, the expressions for $\xi(\theta)$ are

$$\xi_a(\theta) = K\int_{\theta_0}^{\theta} \frac{(df_a/d\theta_1)}{\theta_\infty - \theta_1}\,d\theta, \tag{43a}$$

$$\xi_b(\theta) = \frac{1}{K}\int_{\theta_0}^{\theta} \frac{d\theta_1}{f_b(\theta_1) - f_b(\theta_\infty)}, \tag{43b}$$

where

$$\theta_0 = (\theta_\infty^{\frac{1}{2}} - 2\theta_m^{\frac{1}{2}})^2.$$

From the factors in front of the integrals, it follows that the forward part of the wave is greatly dispersed at large K, while the rearward part is compressed into a small fraction of a radiation mean free path. As shown in Fig. 4, the two branches of $g(\theta)$ intersect at $\theta = \theta_0 \neq 0$. Consequently there is an imbedded adiabatic inviscid shock. This is followed by a region of rapid velocity and temperature variation as in the upper right plot in Fig. 2. The latter variation, taken together with the adiabatic shock, can be interpreted as an imbedded isothermal shock, in the limit of infinite K. The figure indicates that the temperatures immediately ahead of and behind the combined regions are equal.

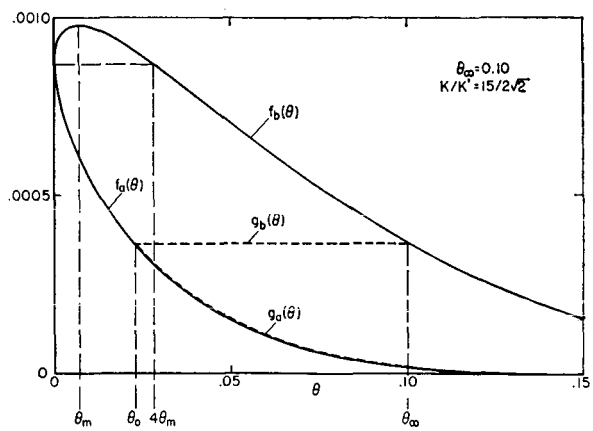

FIG. 4. The functions $f(\theta)$ and $g(\theta)$; $\theta_\infty = 0.10$, $K/K' = 15/2\sqrt{2}$.

Relationship of the Limit $K \to \infty$ to the Rosseland Approximation

In the final section we provide additional details concerning the interrelation between the limiting form of the exact solutions when K increases indefinitely and the Rosseland approximation wherein the radiative heat transfer process is expressed in terms of a thermal heat conduction equation. The latter approximation can be arrived at by taking $T^4(\eta_1)$ in Eq. (7) to be a slowly varying function [i.e., each derivative of $T^4(\eta_1)$ is assumed negligible compared to the derivatives of lower order, including $T^4(\eta_1)$ itself]. After a partial integration Eq. (7) can be written

$$q_r = -2\int_{-\infty}^{\infty} \frac{\partial(\sigma T^4)}{\partial \eta_1} E_3(|\eta - \eta_1|)\,d\eta_1. \tag{44}$$

Since $T^4(\eta)$ is slowly varying, the integral is approximated as follows

$$q_r \approx -2\frac{\partial(\sigma T^4)}{\partial \eta}\int_{-\infty}^{\infty} E_3(|\eta - \eta_1|)\,d\eta_1 = \frac{-4}{3}\frac{\partial(\sigma T^4)}{\partial \eta} = \frac{-16\sigma T^3}{3\alpha}\frac{\partial T}{\partial x}. \tag{45}$$

This expression for the radiative heat flux is of the same form as Fourier's law for thermal heat conduction, $q = -k(\partial T/\partial x)$. Thus the Rosseland approximation leads to the definition of an equivalent heat conduction coefficient k_r such that

$$q_r \approx -k_r\frac{\partial T}{\partial x}, \qquad k_r = \frac{16}{3}\frac{\sigma T^3}{\alpha}. \tag{46}$$

If the approximation

$$E_2(\eta) \approx me^{-n\eta}$$

is used in Eq. (7), the same result is obtained as long as m is taken equal to $\frac{1}{3}n^2$.

Use of Eq. (46) at the outset in place of Eq. (7) leads to

$$(v_1 - v)(v - v_2) = K(v - v^2)^3(d/d\xi)(v - v^2) \quad (47)$$

in place of the integral Eq. (13). It is to be noted that this derivation is based on the assumption that T^4 and hence $(v - v^2)^4$ does not vary appreciably in one radiation mean free path.

Since ξ is essentially in units of the radiation mean free path, the ξ-wise gradient of $(v - v^2)^4$ must be small. But Eq. (47) can be recast in the form

$$\frac{d}{d\xi}(v - v^2)^4 = \frac{4(v_1 - v)(v - v_2)}{K} = \frac{4c_3[(\theta_\infty - \theta)/\theta_\infty^{\frac{1}{2}}]}{K/K'}, \quad (48)$$

where c_3 is $\theta_\infty^{\frac{1}{2}}/K'$ and from Eq. (27) is fixed for a known value of γ. For sufficiently large values of K/K' the magnitude of the right term can be made arbitrarily small and the derivative term on the left is consequently small. This is the basis for the statement that the Rosseland limit corresponds to $K \to \infty$.

These remarks imply that the profiles in the right column of Fig. 2 should be consistent with results obtained from the Rosseland approximation. Our results indicate, however, that this consistency is strictly true only in the case of weak waves and that a singular perturbation effect appears in the limiting condition for intermediate and strong shocks. The singular behavior is exhibited in the internal structure of the imbedded isothermal shocks discussed in the preceding section and pictured in the right column of Fig. 2. The Rosseland approximation leads to Becker's solution for a conducting shock in the absence of radiation and for zero viscosity. This solution includes an imbedded isothermal shock as in the present solution for large K, but with no internal structure. It is not surprising that the internal structure indicated by the integral equation is lost in the Rosseland approximation, since the simplification leading to the approximation requires that v and T be nearly constant in one radiation mean free path, whereas the internal structure based on the refined analysis contains an appreciable variation in a small fraction of a radiation mean free path. It is interesting to note that for a strong shock there is a temperature peak considerably larger than that which would occur in the absence of radiation, see the upper right plot in Fig. 2. This feature is missed entirely by the Rosseland approximation.

APPENDIX: UNIQUENESS OF SOLUTION

In the text it was assumed that the velocity decreases monotonically from the initial to the final value. It will be shown here that, without this restriction, the solution is not unique. However, it will be seen that the nonmonotonic velocity profiles entail a violation of the second law of thermodynamics, and must therefore be excluded.

Equations (20a, b) can be derived from Eq. (13) without assuming v monotonic, provided that the sign of $\pm\theta^{\frac{1}{2}}$ in equations (17) and (18b) is not specified relative to the sign of ξ. In making this change, we shall at the same time express the parameters γ, v_1, and v_2 in terms of the quantities $\theta_m = (\gamma - 1)^2/4(\gamma + 1)^2$, $\theta_\infty = \frac{1}{4}(v_1 - v_2)^2$, previously defined. Then Eqs. (17) and (18b) are replaced by

$$v = \tfrac{1}{2} + \theta_m^{\frac{1}{2}} \pm \theta^{\frac{1}{2}}, \quad (A1)$$

$$F(\theta) = \tfrac{1}{4}K[\tfrac{1}{4} - (\theta_m^{\frac{1}{2}} \pm \theta^{\frac{1}{2}})^2]^4. \quad (A2)$$

The requirements that θ and G be continuous functions of ξ, and hence $G(\theta)$ continuous, remain intact.

Equations (20a, b) combine to form the equation

$$(F - G)\, dG/d\theta = \theta_\infty - \theta \quad (A3)$$

for the unknown function $G(\theta)$. There are two branches of $G(\theta)$ corresponding to the two branches of $F(\theta)$, which in turn correspond to the two branches of $\pm\theta^{\frac{1}{2}}$, appearing in Eqs. (A1) and (A2). The boundary conditions associated with Eq. (A3) are

at $\xi = -\infty$:

$$v = v_1 = \tfrac{1}{2} + \theta_a^{\frac{1}{2}} + \theta_\infty^{\frac{1}{2}}, \quad \theta = \theta_\infty, \quad G = F_a(\theta_\infty); \quad (A4)$$

at $\xi = +\infty$:

$$v = v_2 = \tfrac{1}{2} + \theta_m^{\frac{1}{2}} - \theta_\infty^{\frac{1}{2}}, \quad \theta = \theta_\infty, \quad G = F_b(\theta_\infty); \quad (A5)$$

where the subscript a corresponds to $(+\theta^{\frac{1}{2}})$ and b corresponds to $(-\theta^{\frac{1}{2}})$ in the expression for $F(\theta)$.

Figure 5 is a sketch of the integral curves, $G(\theta)$, for a typical case. That the starting point, 1, and final point, 2, are saddle points follows from a study of equation (A3) in the neighborhood of these points. Equation (A3) shows immediately that the integral curves are monotonic unless they cross the line $\theta = \theta_\infty$ or unless they cross the branch of $F(\theta)$ with which they are associated. A brief study indicates that an integral curve leaving point 1 or point 2 cannot make such a crossing. Thus each of the curves G_a, G_c, G_b, G_d, etc. is monotonic in the range where it is defined. Also, each lies always

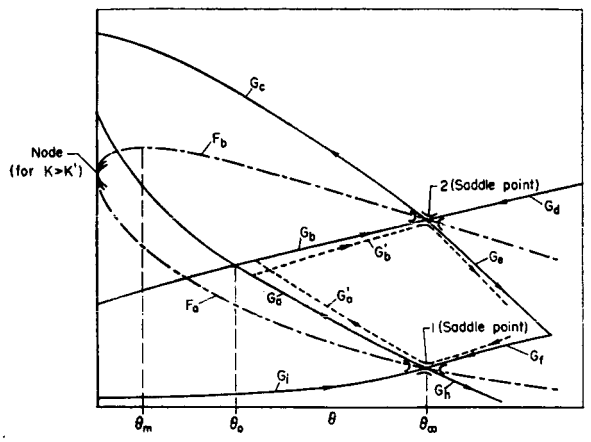

FIG. 5. The integral curves $G(\theta)$.

on the same side of the F curve that it intersects at 1 or 2.

Once the direction of increasing G is known for each curve, the direction of increasing ξ is determined by Eq. (20a), rewritten as

$$dG/d\xi = \theta_\infty - \theta. \tag{A6}$$

The arrows in Fig. 5 have been drawn to correspond to increasing ξ.

We are interested in finding a solution curve from point 1 ($\xi = -\infty$) to point 2 ($\xi = +\infty$). The value of ξ must increase along this path (the direction of the arrows). There is the requirement that $G(\theta)$ be continuous, but the desired solution curve can transfer from one integral curve to another at a point where they intersect. We can conclude that G_h does not intersect any of the other lettered curves, except possibly G_e, on which the arrow is backwards. The arrows are also backwards on G_f and G_i. The only remaining possibility is to start out on G_a. A possible intersection of G_a with G_c is not of interest because of the orientation of the arrow on G_c. If we transfer from G_a to G_b at $\theta = \theta_0$, where the two are equal, and proceed along G_b to point 2, none of the required conditions is violated. Since G_a and G_b are monotonic and hence can intersect at only one point, the solution is unique, if we can exclude multiple transfers involving integral curves that do not pass through points 1 or 2.

Consider the expansion shock represented by the path from point 2 along G_e, a transfer to G_f at the point of intersection, and from there to point 1 along G_f. There are no conditions arising from the integral There are no conditions arising from the integral Eq. (13) that would exclude such a solution. But the transition from G_e to $G_f(-\theta^{\frac{1}{2}}$ changes to $+\theta^{\frac{1}{2}})$ corresponds to an imbedded inviscid adiabatic *expansion* shock, and is excluded by an appeal to the second law of thermodynamics. Thus our system of flow equations must be supplemented by a statement of the second law, as in classical inviscid flow theory.

Returning to the over-all compression wave (initial state at point 1), similar reasoning shows that a velocity profile involving multiple shocks is a solution of the integral Eq. (13). For example, consider the path starting along G_a, a transfer to G_b' at the point of intersection, transfer to G_a', transfer to G_b, and thence along G_b to point 2. No conditions arising from the integral equation are violated by this solution. But the transfer from G_b' to G_a' ($-\theta^{\frac{1}{2}}$ changes to $+\theta^{\frac{1}{2}}$) violates the second law. In any solution involving multiple transfers, every other transfer must correspond to an imbedded inviscid expansion shock. To show this it is only necessary to establish that distinct integral curves associated with the same branch of $F(\theta)$ do not intersect, which follows from a comparison of the slopes indicated by equation (A3). The last statement should be qualified slightly in that such intersections can occur at the node located at $\theta = 0$. But a little reflection reveals that this does not interfere with the final conclusion that the solution along G_a and G_b is unique, if imbedded expansion shocks are not permitted.

Once all other solutions are excluded and ξ is set equal to zero at $v = \gamma/(\gamma + 1) = \frac{1}{2} + \theta_m^{\frac{1}{2}}$, it follows from Eq. (A1) that the sign of $\pm\theta^{\frac{1}{2}}$ coincides with the sign of ξ. Since θ decreases in the transit along G_a (in the direction of the arrow) and increases along G_b, it follows [from equation (A1)] that v is monotonic. Assuming v monotonic at the outset also led to a unique solution. We therefore conclude that this restriction can be interpreted as an imposition of the second law of thermodynamics.